# Fabrication of Supercapacitor Electrodes Using Fluorinated Single-Walled Carbon Nanotubes

**Ji Yeong Lee,[†] Kay Hyeok An,[‡] Jeong Ku Heo,[‡] and Young Hee Lee*[,†,‡]**

*Department of Nanoscience and Nanotechnology and BK21 Physics Division, Center for Nanotubes and Nanostructured Composites, Sungkyunkwan University, Suwon 440-746, Republic of Korea*

*Received: March 3, 2003; In Final Form: May 23, 2003*

We have fabricated electrodes for a supercapacitor using fluorinated single-walled carbon nanotubes (SWCNTs). Although the specific surface areas of the pristine and fluorinated SWCNTs are similar, the electrochemical reactions are different significantly from each other. The specific capacitance of the fluorinated SWCNTs is smaller than that of the pristine sample particularly at large discharge current density, which can be attributed to the micropores formed during fluorination. After heat treatment at 900 °C for 30 min, the nonredox reaction is dominant, and furthermore, the fluorinated sample gives a larger specific capacitance than the pristine sample.

## Introduction

The carbon nanotube (CNT) is a new versatile material that has strong applicabilities to several areas, particularly energy storage such as hydrogen storage,[1] supercapacitors,[2−4] secondary batteries,[5−7] and fuel cells.[8] Superb chemical stability, high conductivity, light mass, large surface area, and flexibility of CNTs provide room to improve storage capacities and even the cycle life of electrodes in supercapacitors and secondary batteries. Despite such advantages, CNTs have not been fully utilized for energy storage devices yet. One of the main reasons is the absence of methods for large-scale synthesis. Another is more critical from both fundamental and technical point of views that the characteristics of CNTs strongly rely on not only the synthetic methods but also the sample preparation conditions. This has been a serious obstacle in energy storage applications. For instance, the hydrogen storage capacity has not been reproducible, although some reported very high capacity.[9] The capacitance in the supercapacitor has been known to vary significantly with the heat treatment of the sample.[4]

The carbon nanotube is a nonpolar material and therefore easily aggregates in polar solvent. This incurs a serious difficulty in fabricating CNT electrodes for energy storage, degrading the performance of electrodes. Therefore, it is desirable to transform the nonpolar CNTs to polar ones if possible. Functionalization of CNT walls by fluorine atoms has been introduced, where atomic and electronic structures were seriously modified.[10,11] An appropriate choice of F content in CNTs is expected to be polar and increase the solubility and wettability in various electrolytes. Yet, the applications of fluorinated CNTs to supercapacitors and secondary batteries have not been reported so far. The purpose of this paper is to fabricate electrodes for supercapacitors using fluorinated CNTs and to investigate their electrochemical properties.

## Experimental Section

Single-walled carbon nanotubes (SWCNTs) were prepared by conventional catalytic arc discharge.[12] The chamber was pumped out to a base pressure of 100 mTorr, and then helium gas was introduced until the pressure reached 100 Torr. The total amount of catalyst in graphite powder was fixed to be 5 wt %, with a fixed ratio of the transition metals (Ni:Co:FeS = 1:1:1), where sulfur was added as a promoter. This increased significantly the yield of CNTs deposited in the chamber. Since there is a chance that the raw samples may differ slightly from batch to batch, several batches were mixed together to increase the reproducibility of the original raw samples. The raw sample contains carbonaceous particles and transition metals. This clothlike raw sample was grinded mechanically and transferred to the reaction chamber for fluorine treatment.

This powder was brought into a Ni boat in the fluorine reaction chamber made by Ni and SUS-316 to prevent erosion. The reaction process is similar to that for carbon fibers.[13] The chamber was pumped out to $10^{-2}$ Torr and purged by nitrogen gases to remove the residual oxygen gases and moisture. $F_2$ gas was then introduced, and the pressure was maintained at 0.2 bar for 10 min for a given reaction temperature of 200 °C. After the reaction, the chamber was pumped out again to $10^{-2}$ Torr and nitrogen gas was refilled prior to the extraction of the powder sample.[14]

The fluorinated SWCNT powder was mixed with a binder. Two different binders were used in our work. The mixture of the F-SWCNTs and poly(tetrafluoroethylene) (PTFE) with a set weight ratio (SWCNT:PTFE = 95:5) was dissolved in isopropyl alcohol (IPA). This SWCNT paste was pelletized and molded onto a Ni foam of 120 pores/in. with a pressure of 1000 psi, followed by an overnight dry in oven.

A unit cell for the capacitor was fabricated with two CNT electrodes separated by a thin polymer (Celgard) in 7.5 N KOH aqueous solution as the electrolyte. The cell was charged at a constant voltage of 0.9 V for 10 min and then discharged at a constant current density of 1−200 mA/g. The discharging capacitance of the test cell was then calculated by $I_{dc}(\Delta t/\Delta V)$, where $I_{dc}$ is the constant discharging current, $\Delta t$ is discharging time, which was measured from 0.54 to 0.45 V in the linear region (about 60−50% of the initial voltage), and the voltage change $\Delta V$ was determined at a constant current discharge.

* Corresponding author. E-mail: leeyoung@skku.edu.
[†] Department of Nanoscience and Nanotechnology.
[‡] BK21 Physics Division.

10.1021/jp034546u CCC: $25.00 
Published on Web 08/02/2003

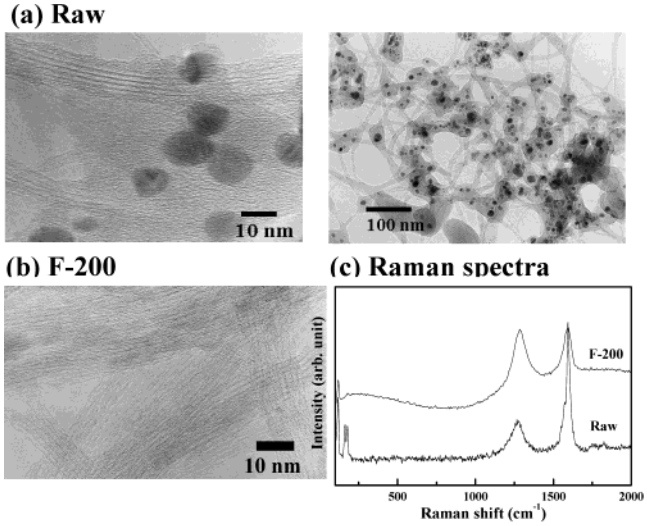


**Figure 1.** (a) TEM images of the as-grown samples in different magnifications and (b) that of the fluorinated sample. The black spots are transition metals. (c) Raman spectra of the raw and fluorinated sample at 200 °C.

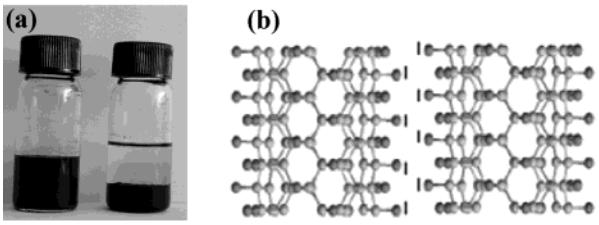


**Figure 2.** (a) Vials containing fluorinated (left) and as-grown SWCNTs (right) in DI water. (b) Ball and stick model for the fluorinated SWCNT wall. Gray and blue balls indicate carbon and fluorine atoms, respectively.

## Results and Discussion

Figure 1 shows the transmission electron microscope (TEM) (JEOL, JEM-3011) images of the as-grown SWCNTs and the fluorinated one. In addition to the SWCNT bundles, the as-grown sample in Figure 1a contains not only the carbonaceous particles but also transition metals (black spots). The CNT walls are preserved after the reaction, although the sample became more resistive.[11] It is interesting to see that some transition metals are removed during fluorine reaction at 200 °C, as can be seen in the clear TEM images in Figure 1b. We speculate that the reactive fluorine gas etches away metal particles.[15] Fluorination of SWCNTs at high reaction temperature leads to disintegrate the tube walls into graphitic layers.[16] Figure 1c shows that the radial breathing mode particularly near 178 $cm^{-1}$ disappears and the defect-related D-band peak intensity near 1250 $cm^{-1}$ becomes larger in the fluorinated sample. This indicates that F-doping creates defects on the tube wall and this trend seems to be more severe in the heavily strained tubes with smaller diameters.[11,16]

To test the solubility, the fluorinated SWCNT powder was dispersed in deionized water. Figure 2 shows pictures of well-dispersed fluorinated SWCNTs in deionized water. The well-dispersed SWCNTs were maintained for several months, whereas the as-grown SWCNTs were sunk at the bottom after several minutes. It is well-known that fluorine atoms form strong bonds with $\pi$ states on the tube walls.[17] A significant charge transfer occurs from the nanotube wall to the fluorine atoms, resulting in partially ionic bonds.[18] This transforms the nonpolar SWCNT to the polar one. Therefore, the polar materials dissolve well in water by incorporating the polar water molecules via dipole−dipole intertactions, as shown in Figure 2b. This property is very advantageous in fabricating electrodes for energy storage devices. We also expect that this may improve the wettability with aqueous electrolytes, which will eventually promote the performance of supercapacitors.

Figure 3 shows $N_2$ adsorption isotherms at 77 K for the raw and fluorinated samples. Both samples show type II adsorption and are not much different from each other. The initial uptake near $0.01P_0$ (atmospheric pressure) indicates the presence of micropores. The gradual increase of the volume adsorbed in the mid pressure range represents the development of various sizes of mesopores. The BET (Brunauer−Emmett−Teller) specific surface area of the as-grown sample is 133 $m^2/g$, relatively small compared to the previously reported ones,[4] which may be attributed to the small bundling sizes, as shown in the TEM images. The average pore diameter is 119 Å. The BET surface area does not change much even in the fluorinated sample. Instead, the micropore area is increased and, hence, the average pore diameter is reduced in the fluorinated sample, as shown in Table 1.

We now test electrochemical properties of the fabricated electrodes. Figure 4 shows typical $V-t$ profiles in terms of discharging currents after charging for 10 min at a constant voltage of 0.9 V. For a complete electric double layer capacitor (EDLC), this curve should be linear. The nonlinear curves in our samples indicate that some redox reaction occurs in the electrodes. Since the samples are not heat-treated, some of the residual oxygen functional groups may remain on the surface, giving rise to the redox reactions. We extract the slope at a voltage interval of 0.54−0.45 V, which is almost linear, to calculate the specific capacitance. At a low discharge current of 10 mA/g, the slope of the raw sample does not change much compared to that of the fluorinated sample. However, the slope becomes sharper at large discharge currents, indicating the reduction of the specific capacitance in the fluorinated sample.

Figure 5a shows the specific capacitance as a function of charging time at a constant charging voltage of 0.9 V. The charging time saturates at about 1 h in both samples. We note that the maximum capacitance of both samples is smaller than

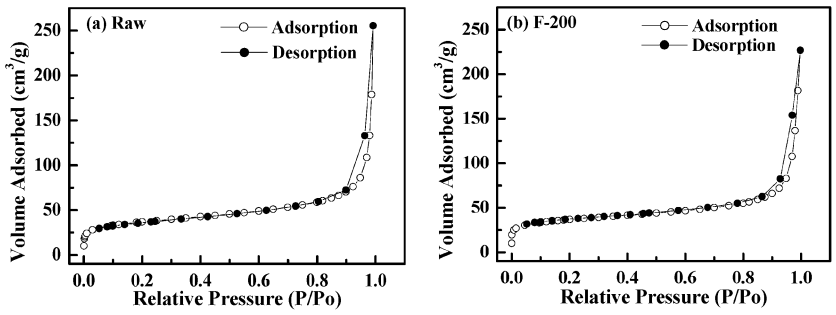


**Figure 3.** $N_2$ adsorption isotherms at 77 K for the raw and fluorinated samples.

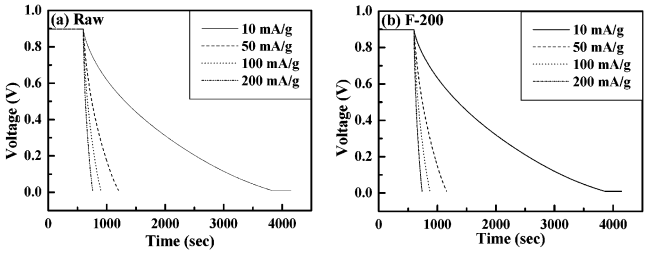


**Figure 4.** $V-t$ profiles of constant voltage charge (0.9 V for 10 min)/ constant current discharge between 0.1 and 0.9 V for (a) the raw and (b) fluorinated samples before heat treatment.

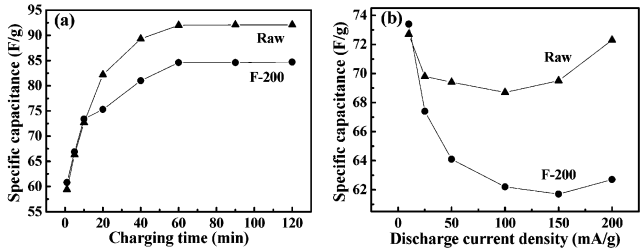


**Figure 5.** (a) Specific capacitance as a function of charging times at a constant charging voltage of 0.9 V for both raw and fluorinated samples with the capacitance measured at a discharge current of 10 mA/g. (b) Specific capacitance as a function of discharge current density after charging at 0.9 V for 10 min.

**TABLE 1: $N_2$ Adsorption Characteristics of the SWCNT Powder**

| | BET area ($m^2$/g) | micropore area ($m^2$/g) | micropore area fraction (%) | micropore vol ($cm^3$/g) | av pore diameter (Å) |
|---|---|---|---|---|---|
| raw | 133 | 78 | 59 | 0.035 | 119 |
| F-200 | 134 | 89 | 66 | 0.039 | 105 |

the previously reported values, where the samples were heat-treated at high temperature.[4] This can be attributed to the low BET surface area (133 $m^2$/g) in our as-grown sample compared to the previous value of 215 $m^2$/g, suggesting that the specific surface area is strongly dependent on the BET surface area. The commercially realizable specific capacitance is 20−50 $\mu$F/$cm^2$ in the electric double-layer capacitor with plane electrodes.[19] For the BET surface area of 133 $m^2$/ g, we can get a rough theoretical estimate of 27−67 F/g in our sample. This value is smaller than the observed maximum value we get from Figure 5a. This is in good contrast with the general belief that the measured value is usually one-fourth of the theoretically estimated one. For instance, commercially available activated carbon gives the specific capacitance of 250 F/g with the BET surface area of 2000−3000 $m^2$/g, which will give a theoretical value of 400−1000 F/g.[19] This unusual increase in the specific capacitance may be attributed to the additional redox reaction due to the residual oxygen gases present on the surface of our electrodes. The raw sample gives larger specific capacitance than the fluorinated sample particularly at large charging times, although the trend should be opposite due to the increase of the micropore area and the decrease in the average pore diameter in the fluorinated sample as shown in Table 1. However, the resistivity also increases in the fluorinated sample,[11] which reduces the specific capacitance of the electrode by increasing the equivalent series resistance in the cell. The specific capacitances at low discharge current density are similar for both samples, whereas these values decrease more rapidly in the fluorinated sample than the raw sample at large discharge currents, as shown in Figure 5b. Abundant micropores with smaller pore diameters are covered by the fluorine ions and can be more easily blocked particularly at large discharge currents. This reduces the specific capacitance.

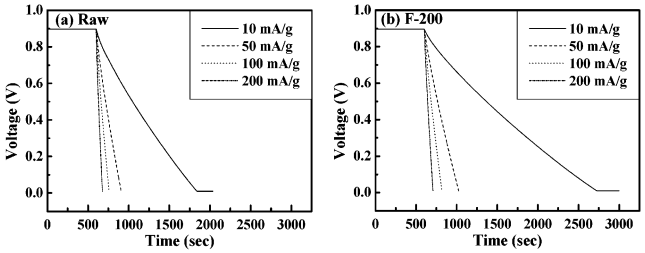


**Figure 6.** Profile of $V-t$ curves after heat treatment at 900 °C for 30 min under He ambient. All other conditions are the same as those in Figure 3.

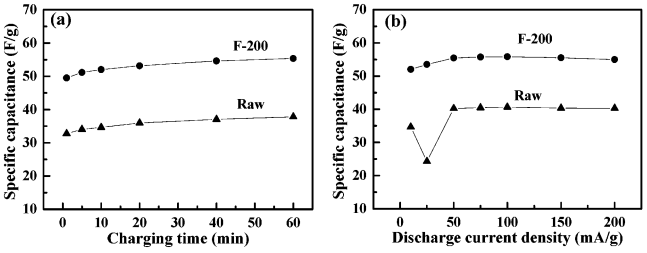


**Figure 7.** (a) Specific capacitance as a function of charging times at a constant charging voltage of 0.9 V for both raw and fluorinated samples after heat treatment at 900 °C for 30 min under He ambient with the capacitance measured at a discharge current of 10 mA/g. (b) Specific capacitance of the heat-treated samples as a function of discharge current density after charging at 0.9 V for 10 min.

Although the redox reaction improves the capacitance, the cycle life of the capacitor is shortened by such a reaction. To improve this, we heated the electrodes at 900 °C for 30 min under He ambient. Figure 6 shows again typical $V-t$ curves of both electrodes. We now see that the curves are perfectly linear except the initial $IR$ drop region. The longer discharging time in the fluorinated sample indicates larger specific capacitance compared to those of the raw sample.

Figure 7a shows the specific capacitance as a function of charging time. The specific capacitances of both heat-treated samples are now lower than those of the untreated samples but certainly remain within the region of theoretically estimated values, which can be attributed to the absence of residual gases on the electrode surfaces. The micropores are expected to be developed due to the fluorine desorption during the heat treatment. The fluorine atoms could be driven off from the side walls of the SWCNTs in forms of $CF_4$, $C_2F_4$, $C_2F_6$, and $COF_2$, resulting in the chemically cut SWCNTs.[20,21] Therefore, the release of fluorine and carbon atoms and the cutting of SWCNTs led to the development of micropores. The resistivity of the electrodes could be also altered due to desorption of fluorine atoms. The fluorinated sample gives consistently larger specific capacitance than the raw sample. We note that the specific capacitance is quite independent of the charging time and the discharge current density, as shown in Figure 7a,b. This characteristic is important from technical point of views that the charging time can be saved and a large power capacitor can be constructed without a significant loss.

## Conclusion

We have investigated the electrochemical properties by fabricating electrodes for supercapacitors using fluorinated SWCNTs. We find that the fluorination of SWCNT walls transforms the nonpolar SWCNTs to the polar ones by forming dipole layers on the walls, resulting in high solubility in

deionized water. Fluorinated samples give lower capacitance than the raw samples before heat treatment. However, after heat treatment, the specific capacitance of the fluorinated samples became higher than those of the raw samples, and furthermore, the specific capacitance was quite independent of the discharge currents of up to 200 mA/g, which is advantageous in practical applications. We find that the specific capacitance is closely related to the specific surface area of the CNT materials and the micropore area.

**Acknowledgment.** This work was supported in part by the Ministry of Science and Technology (MOST) through the National Research Laboratory (NRL) and in part by the Korea Science and Engineering Foundation through the Center for Nanotubes and Nanostructured Composites at SKKU. We acknowledge KBSI (Chonju branch) for their generous hospitality of allowing BET measurement (UPA-150).

## References and Notes

(1) Dillon, A. C.; Jones, K. M.; Bekkedahl, T. A.; Kiang, C. H.; Bethune, D. S. Heben, M. J. *Nature* **1997**, *386*, 377.

(2) Niu, C.; Sichel, E. K.; Hoch, R.; Moy, D.; Tennent, H. *Appl. Phys. Lett.* **1997**, *70*, 1480.

(3) Diederich, L.; Barborini, E.; Piseri, P.; Podesta, A.; Milani, P.; Schneuwly, A.; Gallay, R. *Appl. Phys. Lett.* **1999**, *75*, 2662.

(4) An, K. H.; Kim, W. S.; Park, Y. S.; Choi, Y. C.; Lee, S. M.; Chung, D. C.; Bae, D. J.; Lim, S. C.; Lee, Y. H. *Adv. Mater.* **2001**, *13*, 497.

(5) Wu, G. T.; Wang, C. S.; Zhang, X. B.; Yang, H. S.; Qi, Z. F.; He, P. M.; Li, W. Z. *J. Electrochem. Soc.* **1999**, *146*, 1696.

(6) Frackowiak, E.; Gautier, S.; Gaucher, H.; Bonnamy, S.; Beguin, F. *Carbon* **1999**, *37*, 61.

(7) Lee, S. M.; Park, K. S.; Choi, Y. C.; Park, Y. S.; Bok, J. M.; Bae, D. J.; Nahm, K. S.; Choi, Y. G.; Yu, S. C.; Kim, N. G.; Frauennnheim, T.; Lee, Y. H. *Synth. Met.* **2000**, *113*, 209.

(8) Li, W.; Liang, C.; Qiu, J.; Zhou, W.; Han, H.; Wei, Z.; Sun, G.; Xin, Q. *Carbon* **2002**, *40*, 787.

(9) Hirscher, M.; Haluska, M.; Dettlaff-weglikowska, U.; Quintel, A.; Duesberg, G. S.; Choi, Y. M.; Downes, P.; Hulman, M.; Roth, S.; Stepanek, I.; Bernier, P. *Appl. Phys. A* **2001**, *72*, 129.

(10) Mickelson, E. T.; Chiang, I. W.; Zimmerman, J. L.; Boul, P. J.; Lozano, J.; Liu, J.; Smalley, R. E.; Hauge, R. H.; Margrave, J. L. *J. Phys. Chem. B* **1999**, *103*, 4318.

(11) An, K. H.; Heo, J. G.; Jeon, K. G.; Bae, D. J.; Jo, C.; Yang, C. W.; Park, C.-Y.; Lee, Y. H.; Lee, Y. S.; Chung, Y. S. *Appl. Phys. Lett.* **2002**, *80*, 4235.

(12) Park, Y. S.; Kim, K. S.; Jeong, H. J.; Kim, W. S.; Moon, J.-M.; An, K. H.; Bae, D. J.; Lee, Y. S.; Park, G.-S.; Lee, Y. H. *Synth. Met*. **2002,** *126*, 245.

(13) Collins, P. G.; Zettl, A. *Phys. Rev. B* **1997**, *55*, 9391.

(14) Lee, Y. S.; Cho, T. H.; Lee, B. K.; Rho, J. S.; An, K. H.; Lee, Y. H. *J. Fluorine Chem*. **2003**, *120*, 99.

(15) Hamwi, A.; Alvergnat, H.; Bonnamy, S.; Beguin, F. *Carbon* **1997**, *35*, 723.

(16) An, K. H.; Park, K. A.; Heo, J. G.; Lee, J. Y.; Jeon, K. K.; Lim, S. C.; Yang, C. W.; Lee, Y. S.; Lee, Y. H. *J. Am. Chem. Soc.* **2003**, *125*, 3507.

(17) Bettinger, H. F.; Kudin, K. N.; Scuseria, G. E. *J. Am. Chem. Soc.* **2001**, *123*, 12849.

(18) Park, K. A.; Choi, Y. S.; Kim, C. W.; Lee, Y. H. *Phys. Rev. B* **2003**, in press.

(19) Conway, B. E. *Electrochemical Supercapacitors: Scientific Fundamentals and Technological Applications*; Kluwer Academic/Plenum Publishers: New York, 1999.

(20) Mickelson, E. T.; Huffman, C. B.; Rinzler, A. G.; Smalley, R. E.; Hauge, R. H.; Margrave, J. L. *Chem. Phys. Lett.* **1998**, *296*, 188.

(21) Gu, Z.; Peng, H.; Smalley, R. E.; Margrave, J. L. *Nano Lett*. **2002**, *2*, 1009.